ISBN: 978-3-95450-208-0 doi:10.18429/JACoW-IPAC2019-WEYYPLS2

FIRST EXPERIMENTAL MEASUREMENTS OF THE CAUSTIC NATURE OF TRAJECTORIES IN BUNCH COMPRESSORS

T.K. Charles*[1,2], J. Björklund Svensson[3], A. Latina[1], S. Thorin[4],
[1] Beams Department, CERN, 1211, Geneva 23, Switzerland
[2] School of Physics, University of Melbourne, 3010, Victoria, Australia
[3] Department of Physics, Lund University, P.O. Box 118, SE-22100, Lund, Sweden
[4] MAX IV Laboratory, Lund, Sweden

Abstract

Advancements in the theory describing density perturbations in accelerated charge particle beams, known as caustics, has been gathering interest over the past few years. This proceeding describes the first experimental measurements of the caustic nature of charged particle trajectories in a particle accelerator. Caustics by their nature are discontinuities that result from small continuous perturbations of an input. Under certain conditions, small density modulations will reliably produce striking changes in the corresponding output current profile. These current modulations can shift along the bunch with varying higher-order longitudinal dispersion. The MAX IV linac double-bend achromats provide the perfect test bed for experimentally verifying how the caustic lines evolve. The natural amplification of small perturbations makes caustics an attractive diagnostic tool, and effective tool for characterise the bunch compressors. This approach also allows us to modify and improve the longitudinal charge profile, removing current spikes or creating tailor shaped current profiles.

INTRODUCTION

Caustics are the coalescence of trajectories forming points, lines or surfaces of greatly enhanced charge density. Often referred to as 'natural focusing' [1], caustics are the envelope of particle trajectories. Figure 1 illustrates a caustic line forming where multiple electron trajectories coalesce. Longitudinal dispersion that can be used to compress a chirped bunch, can lead to caustics evidenced by current spikes at the head or tail, or both the head and tail of a bunch.

A caustic expression has been derived based upon the approach presented in reference [2]. This parametric expression describes the longitudinal position of the caustics for a given set of control parameters, R_{56}, T_{566}, and U_{5666} (i.e. the first-, second-, and third-order longitudinal dispersion);

$$\tilde{z}(z_i) = -z_i - \frac{R_{56}\delta(z_i)}{2} + \frac{U_{5666}\,\delta^3(z_i)}{2} + \frac{\delta(z_i)}{2\delta'(z_i)} \quad (1a)$$

$$\tilde{T}_{566}(z_i) = \frac{1}{2\delta(z_i)}\left(-R_{56} - \frac{1}{\delta'(z_i)} - 3U_{5666}\,\delta^2(z_i)\right) \quad (1b)$$

where $\delta(z_i)$ is the shape of the initial longitudinal phase space distribution (or chirp), often described by a high-order polynomial and $\delta'(z_i)$ is the derivative with respect to z_i.

* tessa.charles@cern.ch

When a bunch is subjected to strong bunch compression, often the compressed bunch will exhibit a single-spike [3–5] or double-horned [6–10] current profile . These current spikes are detrimental to FEL performance, leading to greater CSR which can increase the horizontal projected emittance [11–13].

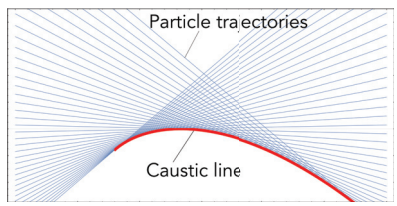

Figure 1: Illustration of a caustic line (red, bold), which is the envelope of particle trajectories (blue) which are focused and defocused by beam optics. Each trajectory that contributes to the caustic, makes a tangent to the caustic line.

In this paper, we present the preliminary work done for measuring of the caustic nature of electron trajectories passing through a dispersive region. The experimental setup is described and some initial results presented.

General Layout of the MAX IV Linac

The MAX IV facility consists of a 300 m S-band linac [14], that provides both full energy and top-up injection to two storage rings (1.5 and 3 GeV) and is a high brightness driver for a short pulse facility (SPF) [4]. Plans are also under way for an Soft X-ray Laser (SXL) beamline fed by the same linac [15]. A 1.6 cell photo cathode gun capable of producing an emittance of 0.4 mm mrad [4] is used for the SPF and for the measurements shown in the next sections. A schematic layout of the linac can be seen in Fig. 2.

Bunch Compressors

Bunch compression is shared across two double-bend achromats. The double achromat is characterized by a positive R_{56} value, and therefore necessitates acceleration on the falling slope of the RF crest. The double achromat design also has a positive T_{566} value which is naturally close to the optimal T_{566} for linearization of the longitudinal phase space. As such, these achromat designs are called "self-linearizing", and avoid the need for a harmonic linearizating cavity [16, 17]. Two weak sextupoles are located in each bunch compressor, positioned in the middle of the achromat where the horizontal dispersion is greatest. These sextupoles

ISBN: 978-3-95450-208-0 doi:10.18429/JACoW-IPAC2019-WEYYPLS2

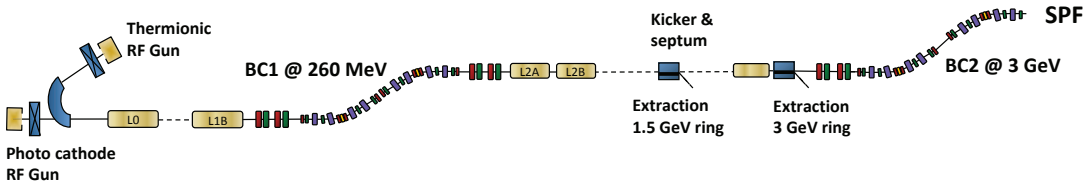

Figure 2: Layout of the MAX IV linac.

allow for fine tuning of the T_{566}. For most operating conditions (i.e. RF phases), the optimal T_{566} is less than the natural T_{566} of the achromat. The sextupoles allow for T_{566} to be reduced for optimal linearization of the longitudinal phase space. The experimental measurements presented in this paper concern BC1, and therefore the optics and parameters of only BC1 are shown in Fig. 3. For the details of BC2, see reference [16].

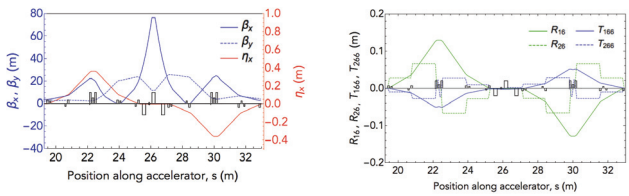

(a) (b)

Figure 3: Optics through BC1. (a) horizontal and vertical beta functions, as well as the horizontal dispersion. (b) first- and second-order dispersion properties along BC1.

It can be noted that the whilst the second-order transverse dispersion does not go to zero at the end of the first achromat, the two achromats making up the bunch compressor exhibit a symmetry whilst bending in the opposite direction (see Fig. 2), and this allows for the second-order transverse dispersion to go to zero at the end of the compressor.

ZERO-CROSSING METHOD

A transverse deflecting cavity is currently planned to be installed at the end of the MAX IV linac this summer [18]. In the meantime, in order to probe the longitudinal phase space and current profile, a modified version of the zero-crossing method was used [17, 19, 20], which allows for measurement of femto-second bunches and give an indication of the current profile shape. The bunch was accelerated off-crest in the main linac and viewed on a screen at maximum dispersion in BC2 [20]. Accelerating off-crest induces a chirp (correlation between energy and position along the bunch), and the horizontal dispersion, η_x, in BC2 streaks the bunch horizontally, making the profile measured in the horizontal plane across the screen proportional to the longitudinal charge profile of the bunch. With the horizontal dispersion at the screen known to be 0.35 m, the width of the pulse on the screen can be related to the energy spread of the beam. This mapping of the transverse position on the YAG screen, Δx, to longitudinal position can be written down as,

$$\Delta t = \frac{\Delta x}{\tan(\phi)\ \omega\ \eta_x} \tag{2}$$

where ω is the RF angular frequency, and ϕ is the RF phase.

Using this approach the bunch length was approximated to range from 665 fs to 1 ps over the measurements presented later in Fig. 6. Bunch lengths as short as 18 fs RMS have been achieved with only one of the linac's two bunch compressors.

The beam was accelerated 40° off crest in the main linac, between BC1 and BC2. The sextupoles were scanned through their range from 0 to 74 m^{-3}. To minimise the contribution of the longitudinal measurement from the transverse plane, the beam was brought to a beta focus at the position of the screen.

The longitudinal wakefields encountered after BC1 induce an additional energy spread in the bunch which will impact the zero-crossing method results [21]. As the energy spread induced by wakefields is dependent upon the bunch length and charge profile shape, we have not attempted correct for this, but rather opted to include conservative error bars to encompassing the effect of wakefields.

Varying the achromat sextupole strengths, varies the T_{566} value linearly, whilst keeping R_{56} constant. By scanning through the range of sextupole strengths, the current profile can be measured on the YAG screen to give an indication of the longitudinal charge profile.

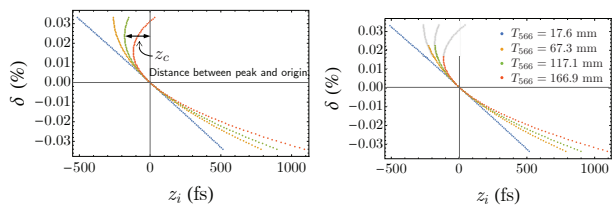

(a) (b)

Figure 4: Longitudinal phase space distribution sketch showing the effect of T_{566}. The evaluation of caustic data points is valid when the curved tail of the phase space distribution remains to the left of the origin. As T_{566} is decreased, the distribution is curved to a greater degree (red curve).

The caustic line of Eq. (1), measures the distance from the peak to the origin, as indicated in Fig. 4a. When the phase space is only partially curved (e.g. the orange or green plots in Fig. 4a), the origin can be determined as the distance from one edge to where the accumulated integrated charge reaches half of the total charge. This approach becomes inaccurate

ISBN: 978-3-95450-208-0 doi:10.18429/JACoW-IPAC2019-WEYYPLS2

once the phase space has curved to the point where the tail of the bunch passes the origin (e.g. the red curve in Fig. 4a).

When the phase space distribution is multi-valued in z, this leads to an artificial increase in the width of the measured current profile. Figure 4b illustrates why this is the case. Ideally, particles at the same longitudinal position, z, should be mapped to the same position on the screen in BC2. However the grey portions of the curve have higher energies than their counterparts of the same longitudinal position, and are therefore mapped to larger values in x on the screen. This makes the distribution broader than it ought to be, and the uncertainty becomes larger for increasing curvature of the phase space distribution. This uncertainty, plus the influence of longitudinal wakefields, are responsible for the offset between the theoretical and experiential results shown in the following section.

RESULTS AND DISCUSSION

By tuning the sextupoles to over- or under-linearize the longitudinal phase space, the position of the current peak can be shifted towards either the head or the tail of the bunch. A detailed explanation of how the sextupoles influence the current profile shape can be found in Reference [2]. Figure 5 shows the current profiles for two sextupole settings, producing a linearly-rising, and a linearly-falling profile.

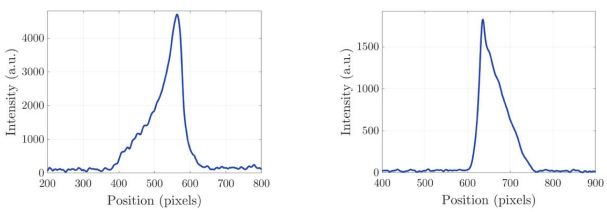

(a) (b)

Figure 5: Current profiles obtained for two different settings for the BC1 sextupoles; a) k2 = 11 m^{-3} and b) k2 = 33 m^{-3}.

Figure 6 shows the evaluation of the caustic line from the YAG screen projections. Good agreement can be seen between the shape of the theoretical expression and the experimental data. However the theoretical and the experimental data are offset by 14 μm. This is most likely due to the imprecise translation of the curved longitudinal phase space distribution from longitudinal to transverse position mentioned above. The analytical expression (red curve in Fig. 6) was calculated using the known values of R_{56}, and T_{566}, and through fitting c_1 and c_2 to the experimental data.

For T_{566} values where Eq. (1) is undefined, caustic current spikes are not expected to appear. Over these regions, the longitudinal phase space is considered well linearized, resulting in a short bunch with a symmetrical current profile.

OUTLOOK

Transverse deflecting Structures (TDS) have proven immensely valuable when it comes to measuring longitudinal phase space distributions [22]. Facilities such as SLAC [23],

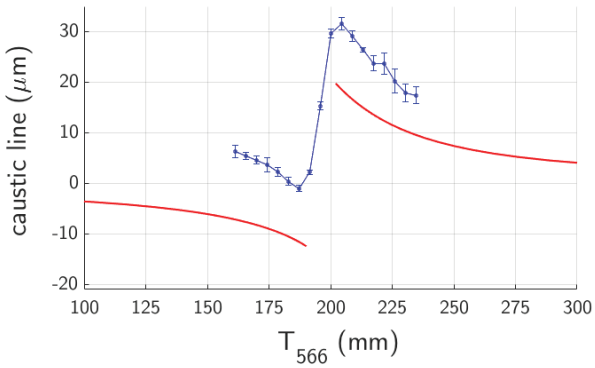

Figure 6: Caustic line analytical expression, Eq. (1) (red line) and experimental data (blue).

FERMI@Elettra [24] and SwissFEL [25] have all demonstrated the usefulness of transverse deflecting cavities. MAX IV has plans under way to install a TDS in at diagnostics beamline at the end of the linac [18]. Once installed, measurements such as the ones presented in this paper, can be repeated with improved temporal resolution and accuracy. It is also expected that the offset visible in Fig. 6 would not be seen with TDS measurements. In addition to the TDS, an up-grade of the photocathode electron gun is being planned [26], which is expected to improve the beam quality and will allow for increased repetition rate.

The production and control of linearly ramped current profiles shown in this paper, is of interest for plasma-based acceleration schemes [27]. The positive gradient linearly ramped profiles of driver beams creates efficient drives the plasma wave [28–30], and negative gradient linearly ramped witness bunches allows for efficient extraction of energy from the wave, as well as minimizes energy spread [30, 31].

Finally caustics has also been applied to longitudinal phase space management of recirculation machines [32] for optimal acceleration and energy recovery.

CONCLUSION

Preliminary results show good agreement in shape between the experimental data and the theory of caustics forming in particle trajectories. An offset between the theoretical expression and the experimental data is observed, which can be accounted for by the indirect mapping of longitudinal position to the measured transverse position on the screen when there is curvature in the longitudinal phase space distribution shape. In addition to validating the caustic expressions, these measurements demonstrate the effectiveness of optical linearization of the MAX IV bunch compressors.

ACKNOWLEDGEMENTS

The authors would like to thank and acknowledge Joel Anderson for creating a realistic bunch distribution exiting the gun, that was used in particle tracking simulations. T.K. Charles acknowledges the financial support of the veski Victoria Fellowship.

ISBN: 978-3-95450-208-0 doi:10.18429/JACoW-IPAC2019-WEYYPLS2

REFERENCES

[1] J. F. Nye, "Natural Focusing and the Fine Structure of Light," *IOP Publ.*, 1999.

[2] T. K. Charles, D. M. Paganin, and R. T. Dowd, "Caustic-based approach to understanding bunching dynamics and current spike formation in particle bunches," *Phys. Rev. Accel. Beams*, vol. 19, no. 104402, 2016.

[3] S. Huang, Y. Ding, Z. Huang, and J. Qiang, "Generation of stable subfemtosecond hard x-ray pulses with optimized nonlinear bunch compression," *Phys. Rev. ST AB*, vol. 17, no. 120703, 2014.

[4] S. Werin, S. Thorin, M. Eriksson, and J. Larsson, "Short pulse facility for MAX-lab," *Nucl. Instr. Meth. Phys. Res. A*, vol. 601, pp. 98–107, mar 2009.

[5] B. Marchetti, M. Krasilnikov, F. Stephan, and I. Zagorodnov, "Compression of a 20 pC e-bunch at the European XFEL for single spike operation," *Phys. Procedia*, vol. 52, pp. 80–89, 2014.

[6] T. K. Charles, D. M. Paganin, A. Latina, M. J. Boland, and R. T. Dowd, "Current-horn suppression for reduced coherent-synchrotron-radiation- induced emittance growth in strong bunch compression," *Phys. Rev. Accel. Beams*, vol. 20, no. 030705, 2017.

[7] J. Arthur, *et al.*, "Linac Coherent Light Source (LCLS) Conceptual Design Report," *SLAC-R-593*, 2002.

[8] B. Beutner, "Longitudinal Design and RF Stability Requirements for the SwissFEL Facility", in *Proc. 4th Int. Particle Accelerator Conf. (IPAC'13)*, Shanghai, China, May 2013, paper WEPFI057, pp. 2821–2823.

[9] S. Di Mitri *et al.*, "Beam Physics Highlights of the FERMI@ELETTRA Project", in *Proc. 37th ICFA Advanced Beam Dynamics Workshop on Future Light Sources (FLS'06)*, Hamburg, Germany, May 2006, paper WG313, pp. 3–5.

[10] Y. Kim *et al.*, "Start-To-End Simulations for PAL XFEL Project", in *Proc. 26th Int. Free Electron Laser Conf. & 11th FEL Users Workshop (FEL'04)*, Trieste, Italy, Aug.-Sep. 2004, paper MOPOS18, pp. 151–154.

[11] Y. Ding, *et al.* "Beam shaping to improve the free-electron laser performance at the Linac Coherent Light Source," *Phys. Rev. Accel. Beams*, vol. 19, no. 100703, 2016.

[12] F. Zhou *et al.*, "Measurements and analysis of a high-brightness electron beam collimated in a magnetic bunch compressor," *Phys. Rev. ST AB*, vol. 18, no. 050702, 2015.

[13] S. Di Mitri and M. Cornacchia, "Electron beam brightness in linac drivers for free-electron-lasers," *Phys. Rep.*, vol. 539, pp. 1–48, 2014.

[14] S. Thorin *et al.*, "The MAX IV Linac", in *Proc. 27th Linear Accelerator Conf. (LINAC'14)*, Geneva, Switzerland, Aug.-Sep. 2014, paper TUIOA03, pp. 400–403.

[15] S. Werin *et al.*, "The Soft X-Ray Laser Project at MAX IV", in *Proc. 8th Int. Particle Accelerator Conf. (IPAC'17)*, Copenhagen, Denmark, May 2017, pp. 2760–2762.

[16] S. Thorin *et al.*, "Bunch Compression by Linearising Achromats for the MAX IV Injector", in *Proc. 32nd Int. Free Electron Laser Conf. (FEL'10)*, Malmö, Sweden, Aug. 2010, paper WEPB34, pp. 471–474.

[17] S. Thorin *et al.*, "Experience and Initial Measurements of Magnetic Linearisation in the MAX IV Linac Bunch Compressors", in *Proc. 38th Int. Free Electron Laser Conf. (FEL'17)*, Santa Fe, NM, USA, Aug. 2017, pp. 273–275.

[18] D. Olsson, F. Curbis, E. Mansten, S. Thorin, and S. Werin, "Transverse RF Deflecting Structures for the MAX IV LINAC", in *Proc. 9th Int. Particle Accelerator Conf. (IPAC'18)*, Vancouver, Canada, May 2018, pp. 3684–3687.

[19] D. X. Wang, G. A. Krafft, and C. K. Sinclair, "Measurement of femtosecond electron bunches using a rf zero-phasing method," *Phys. Rev. E - Stat. Physics, Plasmas, Fluids, Relat. Interdiscip. Top.*, vol. 57, no. 2, pp. 2283–2286, 1998.

[20] F. Curbis, O. Karlberg, S. Thorin, and S. Werin, "Prospects for Longitudinal Phase-space Measurements at the MAX IV Linac", in *Proc. 5th Int. Particle Accelerator Conf. (IPAC'14)*, Dresden, Germany, Jun. 2014, pp. 3665–3667.

[21] Z. Huang, K. Bane, Y. Ding, and P. Emma, "Single-shot method for measuring femtosecond bunch length in linac-based free-electron lasers," *Phys. Rev. ST AB*, vol. 13, no. 092801, pp. 1–9, 2010.

[22] C. Behrens, *et al.* "Few-femtosecond time-resolved measurements of X-ray free-electron lasers," *Nature Communications*, vol. 5, no. 3762, pp. 1–7, 2014.

[23] P. Emma, R. Akre, L. Bentson, and P. Krejcik, "Bunch Length Measurements Using a Transverse RF Deflecting Structure in the SLAC Linac", in *Proc. EPAC'02*, Paris, France, Jun. 2002, paper THPRI097, pp. 1882–1884.

[24] M. Veronese *et al.*, "Longitudinal Electron Beam Diagnostics for the FERMI@Elettra FEL", in *Proc. 15th Beam Instrumentation Workshop (BIW'12)*, Newport News, VA, USA, Apr. 2012, paper THAP02, pp. 259–263.

[25] P. Craievich, R. Ischebeck, F. Loehl, G. L. Orlandi, and E. Prat, "Transverse Deflecting Structures for Bunch Length and Slice Emittance Measurements on SwissFEL", in *Proc. 35th Int. Free Electron Laser Conf. (FEL'13)*, New York, NY, USA, Aug. 2013, paper TUPSO14, pp. 236–241.

[26] J. Andersson *et al.*, "The Pre-Injector and Photocathode Gun Design for the MAX IV SXL", presented at the 10th Int. Particle Accelerator Conf. (IPAC'19), Melbourne, Australia, May 2019, paper TUPTS061, this conference.

[27] J. Björklund Svensson, *et al.*, "Beamline Design for Plasma-Wakefield Acceleration Experiments at MAX IV," *2018 IEEE Adv. Accel. Concepts Work.*, pp. 1–4, 2018.

[28] K. L. F. Bane, P. Chen, and P. B. Wilson, "On Collinear Wakefield Acceleration," *SLAC-PUB-3662*, 1985.

[29] P. Chen, J. J. Su, J. M. Dawson, K. L. Bane, and P. B. Wilson, "Energy transfer in the plasma wake-field accelerator," *Phys. Rev. Lett.*, vol. 56, no. 12, pp. 1252–1255, 1986.

[30] K. V. Lotov, "Efficient operating mode of the plasma wake-field accelerator," *Phys. Plasmas*, vol. 12, no. 053105, pp. 1–4, 2005.

[31] M. Tzoufras *et al.*, "Beam loading in the nonlinear regime of plasma-based acceleration," *Phys. Rev. Lett.*, vol. 101, no. 145002, pp. 1–5, 2008.

[32] T. K. Charles, D. Douglas, and P. H. Williams, "Applications of Caustic Methods to Longitudinal Phase Space Manipulation", in *Proc. 9th Int. Particle Accelerator Conf. (IPAC'18)*, Vancouver, Canada, Apr.-May 2018, pp. 1790–1793.